

seqKAN: Sequence processing with Kolmogorov-Arnold Networks

Tatiana Boura and Stasinios Konstantopoulos

Institute of Informatics and Telecommunications,
NCSR ‘Demokritos’, Ag. Paraskevi, Greece
{tatianabou, konstant}@iit.demokritos.gr

Abstract.

Kolmogorov-Arnold Networks (KANs) have been recently proposed as a machine learning framework that is more interpretable and controllable than the multi-layer perceptron. Various network architectures have been proposed within the KAN framework targeting different tasks and application domains, including sequence processing. This paper proposes seqKAN, a new KAN architecture for sequence processing. Although multiple sequence processing KAN architectures have already been proposed, we argue that seqKAN is more faithful to the core concept of the KAN framework. Furthermore, we empirically demonstrate that it achieves better results. The empirical evaluation is performed on generated data from a complex physics problem on an interpolation and an extrapolation task. Using this dataset we compared seqKAN against a prior KAN network for timeseries prediction, recurrent deep networks, and symbolic regression. seqKAN substantially outperforms all architectures, particularly on the extrapolation dataset, while also being the most transparent.

Keywords: seqKAN, Machine Learning, Kolmogorov-Arnold Networks, KAN, Timeseries Processing

1 Introduction

Kolmogorov-Arnold Networks (KANs) were recently proposed by Liu et al. [5] as an alternative machine learning framework to the ubiquitous *multi-layer perceptron (MLP)*. KANs introduce the idea that if edge weights are lifted to learnable functions, this suffices to capture non-linearities in the data so that nodes can simply sum incoming edges. This idea is inspired by the *Kolmogorov-Arnold Representation Theorem (KAT)* that proves that any multi-variate function can be re-formulated using two layers of uni-variate functions and simple (unweighted) summation.

KAT has been the object of an extensive discussion regarding its relevance to machine learning, summarized by Schmidt-Hieber [6]. One notable point in this discussion is that KAT guarantees the existence of uni-variate functions that can be combined into an exact representation any multi-variate function, but offers neither a construction nor any guarantee on the properties of these uni-variate functions other than being continuous. In fact, with the exception of trivial cases, these functions are suspected to be highly non-smooth and practically impossible to construct either analytically or empirically.

The KAN architecture circumvents objections to KAT’s relevance to machine learning by framing KANs as *approximators* (as opposed to KAT’s exact representations) that stack two *or more* layers. This re-contextualization into the modern deep learning environment has

mustered impressive interest from the machine learning community with more than 10 extensions and applications published within the few months since the original KAN article [1, Section 1].

In this paper we present *seqKAN*, a new architecture within the KAN framework for processing sequences. Our main contribution is that this architecture is more faithful to the core concept of the KAN framework as it avoids re-introducing weighted summation and fixed activation function in the form of conventional MLP-styled recurrency cells. A secondary contribution is the definition of a new evaluation task that has several characteristics (lacking from existing tasks) geared towards combining quantitative evaluation with a qualitative analysis of the results. In the remainder of this article we will first provide the relevant background on KANs and their recurrent extensions (Section 2) and then present seqKAN (Section 3). We will then present and discuss the evaluation task and our experimental results (Section 4) and finally close with conclusions and directions for future work (Section 5).

2 Background

2.1 Kolmogorov-Arnold networks

As mentioned above, the basic idea underlying KANs is that the activation functions that transform values as they move forward through layers are learned from the data and not pre-determined; and that each node in a layer performs simple addition (without weights) over the values it receives from each node of the preceding layer. Figure 1 gives a characteristic example of how values from a 3-node layer propagate to a 2-node layer.

Each *activation function* $\phi_i(\cdot)$ is the weighted sum of a learned spline and $\text{silu}(x) = x/(1 + \exp(-x))$. That is:

$$\phi_i(x) = w_1 \cdot \text{silu}(x) + w_2 \cdot \text{spline}_i(x)$$

where w_1, w_2 and spline_i need to be trained for each edge of the network. The original publication explains w_1, w_2 as implementation details that make the network well-optimizable [5, p. 6]. Besides completely learned splines, activation functions can also be parameterized prior functions. In this case, the user provides univariate function implementations which the network parameterizes via affine transformations (translation and scaling) to fit the data.

By comparison to a conventional neural network, KANs have significantly more parameters to train. Assuming the same number of nodes and edges, a NN learns a single weight for each incoming edge of each node. A KAN, by comparison, learns w_1, w_2 and the spline

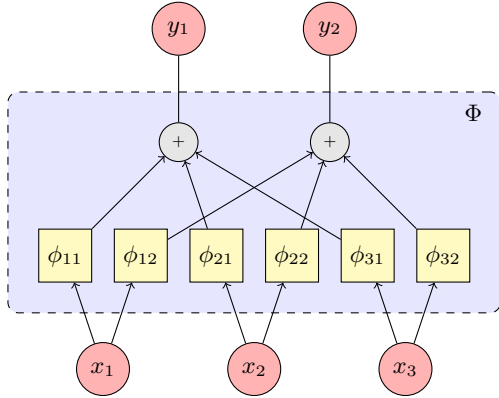


Figure 1: An example of a 2-layer KAN with three input nodes fully connected to two output nodes. The value at each input node is passed to two activation functions, one for each output node. For instance, for input node x_1 , there are two ϕ_{1x} activation functions: ϕ_{11} contributes to output node y_1 and ϕ_{12} contributes to output node y_2 . The value at each output node is the sum of the results of the corresponding activation functions. So the value of output node y_1 is $\phi_{11}(x_1) + \phi_{21}(x_2) + \phi_{31}(x_3)$ and the value of y_2 is $\phi_{12}(x_1) + \phi_{22}(x_2) + \phi_{32}(x_3)$.

parameters or the translation/scaling parameters for each edge. As a consequence, KANs are a viable alternative only when they can adequately approximate the target function with considerably fewer and narrower layers, resulting in significantly fewer edges. When seen under this light, KANs are a significantly *less distributed* representation than NNs. This is further emphasised by the fact that the loss function biases training towards *sparsity*, that is, towards having as few nodes as possible receive non-zero inputs and produce non-zero outputs. Naturally, nodes with almost-zero inputs and outputs are pruned to improve readability with minimal impact on network performance. This technique is similar to regularization in MLPs, but in KANs the result is directly interpretable.

The above make KANs both better *interpretable* and more directly *controllable*. Interpretability basically boils down to the fact that multiple parameters are lumped together into a spline, which can be easily visualized as a function graph and understood by the operator as a familiar function. This greatly reduces the number of different objects and interactions between them that need to be absorbed by a human operator in order to understand what has been learned. Controllability in KANs has multiple facets: from the ability to provide prior functions besides the learned ones, to the ability to replace a familiar-looking spline with a known function, to the ability to prune dependencies that appear to be overfitting or, in general, not capturing the underlying phenomenon.

2.2 Processing sequence data

There are two major approaches in processing sequences: Those receiving the complete sequence as input and those receiving the sequence one datapoint at a time. In the former case the system uses the position in the input vector or, in some cases, an explicit time representation to encode temporal relationships. The *Transformer* architecture [8] is a prime example of this approach, where *attention* is trained to weigh past tokens that are pertinent to the processing of the current token.

Investigating how the concepts of attention and KAN can be integrated can potentially give fruitful results, but the current KAN

literature only includes extensions of *Recurrent Neural Networks (RNN)* and, in fact, of LSTM networks. The *Long Short-Term Memory (LSTM)* [4] and the *Gated Recurrent Unit (GRU)* [2] architectures are examples of the more specific family of architectures within the RNN framework where *gates* are trained to control the flow of information to and from a *hidden state* that distills the effect of past inputs on the processing of the current input.

The most mature among these initial approaches to utilizing KANs for sequence processing is the *Temporal Kolmogorov-Arnold Network (TKAN)* [3]. TKAN replaces the output layer of the LSTM cell with an array of KANs, each of which KANs itself comprises multiple KAN layers. The outputs of these KANs are combined into a single vector through trainable weights. This combined vector includes (a) a recurrent input that is fed back into both the LSTM cell and the KAN layers, and (b) the output of the TKAN layer. These layers are then stacked to form a TKAN network.

3 seqKAN

Our seqKAN architecture introduces recurrency directly into the KAN architecture without adding structures that rely on trained weights and fixed activation functions. This makes seqKAN more faithful to the core concept of the KAN framework, and more capable of fully exploiting the interpretability and controllability offered by KANs.

By contrast, the way TKAN integrates KAN layers within the LSTM cell *and* also uses trained weights to combine values leaves a good part of the overall TKAN architecture on the side of MLP networks and outside the scope of learned activation functions. To a large extent this undermines the value of using a KAN-based architecture: We have no reason to believe that significant pieces of the knowledge distilled from the data will not be stored in the MLP part of the network and become opaque. Furthermore, even the knowledge that is stored in the learned functions will be obfuscated by its interaction with the opaque part of the network offering no opportunities to understand or, even more so, edit and control what has been learned.

This goes beyond TKAN and LSTM and is a more general statement of our core motivation: The choice of activation functions in RNNs is the result of careful consideration and extensive experimentation and has proven itself effective. We have no reason to believe that replacing these activation functions with learnable functions *in the same or a similar network structure* can improve results. If anything, such a move introduces the overhead of fitting splines instead of using the functions that are known to work well.

In order to force the network to store knowledge in the less distributed, more interpretable KAN splines we should develop a KAN architecture that is performant without incorporating MLP structures. Our seqKAN architecture draws inspiration from the RNN architecture but reformulates it in a purely KAN network without trainable weights. seqKAN has one layer that receives input and maps it to a hidden state that is both pushed back to the input and sent to an output layer that computes the outputs (Figure 2).

In the specific configuration used in our experiments, the output layer is a [3,2] KAN layer, identical to the one shown in Figure 1. The output layer Φ_o maps a single-variable hidden state and the two variables from the previous time-step to the two output variables. The hidden-state layer Φ_h is a [3,1] KAN layer that maps the two input variables and the previous hidden state to the new hidden state.

The architectural decision to feed the previous inputs into the output layer is driven by preliminary experiments that compared this architecture against a seqKAN/wide architecture where a wider Φ_h gave the network enough degrees of freedom to learn identity activa-

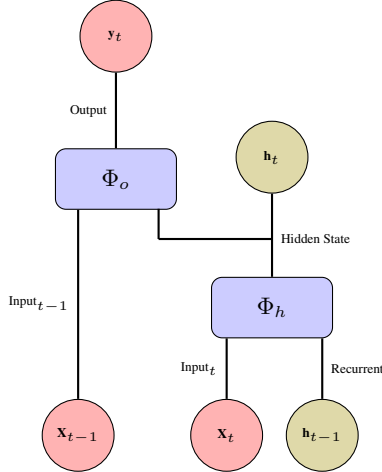


Figure 2: seqKAN architecture. At each timestep, the multivariate input X_t , along with the previous hidden state h_{t-1} , is passed through the hidden-state layer Φ_h , which computes the current hidden state h_t . The current hidden state is then passed through the output layer Φ_o , which computes the current output by also utilizing the multivariate input from the previous timestep, X_{t-1} .

tion functions in Φ_h to simply maintain the previous inputs and pass them to the output layer. In these preliminary experiments seqKAN outperformed seqKAN/wide by a large margin. We will revisit this point in Section 4.2.

4 Experimental Results and Discussion

4.1 Experimental Setup

In order to evaluate seqKAN’s ability to capture temporal dependencies in multivariate time series inputs, we designed a new learning task that has the following characteristics that we have not (cumulatively) found in tasks previously used in the KAN or sequence processing literature:

- It is a multi-variate sequence where the variables interact and affect each other (and, of course, the expected outputs) non-linearly, since the ability to disentangle and elucidate complex dependencies between the input variables is a key promise of KANs.
- It models a non-stationary, evolving phenomenon where a superficial drift can be explained by discovering a long-term trend. Naturally, the interaction between the trend and the outputs should not be simple superposition but a non-linear composition. This tests both the ability to disentangle complex compositions as well as the ability to build models with radically different behaviours in different parts of the variables’ value domains without catastrophic forgetting. This latter aspect, in particular, is meant to test the value KAN extract from fitting splines as opposed to using pre-defined functions.
- It models a well-understood phenomenon and offers itself to an analysis that qualitatively evaluates if the learned network actually models the underlying phenomenon or has chanced upon a solution that fits the available data but is not expected to perform well in corner cases; Noting, of course, that well-understood only implies that the correct computation is known and not that it is straightforward.

Based on the above, we built our task on data from the dynamics of a pendulum where the string gets longer as time progresses, resulting

in motion captured by differential equations without closed-form solutions [9].

More details on the physics of the problem and the exact equations used to generate motion data are given in Appendix A. For our purposes here, it suffices to clarify that string length L depends only on time. But L , the angular displacement θ of the pendulum, and its derivatives angular velocity ω and angular acceleration α form a system of differential equations. This system has no closed-form solution but can be solved numerically by stepping through time from its initial parameters, which makes it appropriate as a sequence processing task since future values can be predicted from previous ones. Specifically, since the equations involve the first two derivatives of displacement, the calculation needs the second order of differences. Therefore from three time steps and L one can calculate the next time step.

However, there is the complication that as the sequence progresses its dynamics change because L changes. By withholding L from the inputs, we create a non-stationary sequence where failure to model the long-term trend will result in considerably higher loss when testing on data extracted from areas of the value space of L not seen during training. In other words, this setup gives the ability to generate an *interpolation* test set where unseen test data can be approximated without capturing the real underlying dynamics and an *extrapolation* test set where such an approximation will result in high loss. We use the exponential function

$$L(t) = 0.1 \cdot \exp_{10}\left(\frac{5.88 \cdot t}{1000}\right)$$

to calculate the length of the pendulum string.¹

From each timestep we extract two binary output variables from the motion parameters: (a) whether the displacement is close to the equilibrium position and (b) whether the energy is increasing or decreasing. The exact definitions are based on lecture notes by Tedrake [7] and also given in Appendix A. Here it suffices to state that the *Close to Equilibrium* label only needs to test whether θ and ω are same-sign or opposite-sign and is straightforward to compute from the sequence whereas the *Energy Increasing* label is a more complex computation also involving L .

Since the two labels share parts of the calculation we expect that combining these labels in a joint learning task helps networks to extract the essential underlying properties of the phenomenon instead of overfitting on a single label. For this reason we defined loss as the mean of the Binary Cross Entropy between the ground-truth value and the value calculated by the network for each of the two labels.

We generated a training set of 200 datapoints, where each datapoint is a sequence of ten $\langle \theta, \omega \rangle$ pairs and the two labels extracted from the motion parameters of the final pair. Similarly, we generated an interpolation test set of 200 datapoints from the same timesteps but with a different initial displacement. Finally, we generated an extrapolation test set of 200 datapoints from timesteps subsequent to the last training datapoint. We chose the sequence length of ten to be considerably longer than the required three, since the systems also need to bring their hidden states to a point where the hidden variable L is estimated from the observed displacement and velocity variables.

To compare the performance of our proposed model, we evaluate it against several sequential data processing models on both interpolation and extrapolation tasks. For baseline performance, we run experiments using an RNN and an LSTM. To compare with a method

¹ In preliminary experiments we compared fixed, linear, and the (actually used) exponential length functions. As expected, the fixed-length task is too easy to make meaningful comparisons. In the linear-length task some differences between systems emerge, but are difficult to discern.

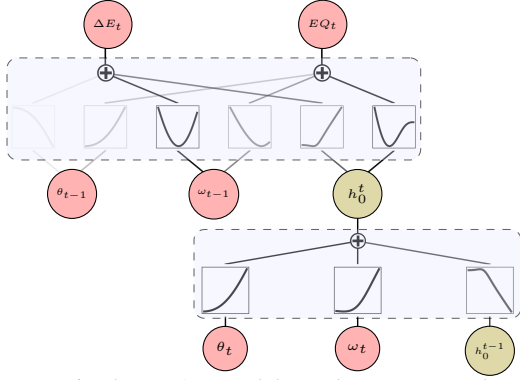


Figure 3: Trained seqKAN model. It takes current and previous ω and θ as inputs, has a single hidden state h_o , and predicts the labels for energy change (ΔE) and equilibrium (EQ). The corresponding ϕ functions are shown with varying opacities, where darker shades indicate a stronger influence on the prediction, while lighter shades signify a diminishing effect.

that explicitly models functions, we employ symbolic regression. Finally, we compare the seqKAN’s performance with the TKAN model to assess different KAN-based architectures. All models are configured to use the same number of parameters.

For our experiments we used the following implementations:

- Our PyTorch implementation of seqKAN, <https://github.com/data-eng/seqKAN>
- The reference implementation of TKAN at <https://github.com/remigenet/TKAN>
- Our PyTorch implementations of RNN and LSTM.
- The PySR 1.3.0 symbolic regressor at <https://github.com/MilesCranmer/PySR>

Our implementations of seqKAN, RNN, and LSTM and of the dataset generator as well as the actual dataset used in the experiments described here can be retrieved from <https://doi.org/10.5281/zenodo.14899652>

4.2 Results with seqKAN

As previously mentioned in Section 3, we tested two variations of the seqKAN architecture in order to establish which one performs better. The seqKAN architecture shown in Figure 2 hard-wires the previous input variables as inputs to the output layer, re-enforcing the effect of the immediately previous input beyond what can be retained in the single-variable hidden-state layer. This optimizes network size at the expense of generality, since we directly allocated learnable functions to treat the immediately previous inputs which we know to be of great relevance.

The more general alternative which we shall call *seqKAN/wide* in the results presented here, is to remove these direct inputs and instead have a wider hidden-state layer. Such a wider layer has the capacity to let two of its functions simply be $y = x$ to allow the previous input to be retained verbatim in the hidden state.

The quantitative results in Table 1 show that seqKAN/wide achieves a significantly lower performance, especially in the most challenging task of predicting the Energy Increasing label in extrapolated datapoints. But the great advantage that the KAN framework is the ability to analyse not only the quantitative results, but also the actual calculations that led to these results. This will give a better understanding of what is observed experimentally.

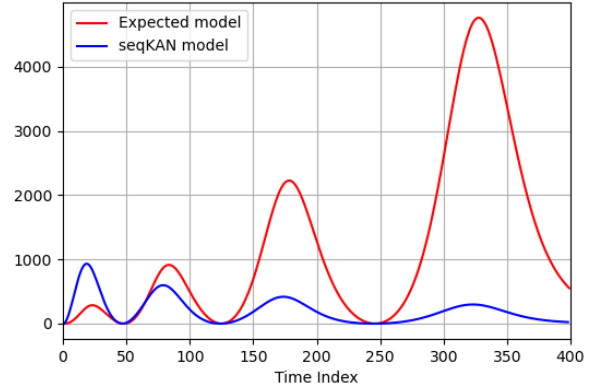


Figure 4: Comparison of the priorly expected model and the model actually learned by seqKAN for the Energy-Increasing label. The seqKAN model is scaled by 10 for plotting clarity.

In our specific case, we can read in Figure 3 that the actual calculation for the Energy-Increase label is an expression along the lines of $\omega_{t-1}^2 + (\Delta\theta_t)^2 + (\Delta\omega_t)^3$, ignoring any scaling that might be encoded in the actual splines and is not visible in the figure. This was derived as follows:

- The ΔE_t node is the sum of a function similar to ω_{t-1}^2 and a function similar to h_o^t for larger time indexes, while the latter term is zeroed out for smaller time indexes.
- The $-\theta_{t-1}$ term is considered inconsequential by the network can be safely ignored. The low significance score is indicated by the very light shade in the figure. At this point it is important to remind the reader that these scores are *not* weights but are used to decide if a term will be included in the sum or completely removed to achieve network sparsity.
- h_o is the sum of three terms: θ_t , ω_t and the opposite of the previous h_o , which in turn adds θ_{t-1} , ω_{t-1} , and the h_o before that. By simply re-arranging the terms, this can be written as $\Delta\theta_t^2 + \Delta\omega_t^3$ and some residue from previous iterations. Noting that the function applied to h_o^{t-1} appears linear but the functions applied to θ_t and ω_t appear polynomial we infer that the network aims at a residue that diminishes the effect of more temporally distant datapoints. So the expression $\Delta(\theta_t + c_1)^2 + \Delta(\omega_t + c_2)^3$ can represent this term.²

As can be seen in Figure 4, there is almost perfect correlation between $\omega_{t-1}^2 + (\Delta\theta_t)^2 + (\Delta\omega_t)^3$ and the expression $(\sin(\theta_t) \cdot \omega_t / \Delta\omega_t)^2$, which is a good approximation of the analytically-derived formula for this label (cf. Appendix A).³ It should be noted that the correlation holds for all the timesteps, including the timesteps beyond 200 where the model extrapolates. In other words, the model has correctly extracted the underlying drift towards ever-increasing pendulum periods as the string gets longer, despite the fact that missing this drift has minimal impact on training loss during the first 200 timesteps.

A reasonable concern would be that we are making this statement from the advantageous position of studying a well-understood phenomenon, and in a more open-ended task we would not have the

² The constants c_1 and c_2 achieve the horizontal translation apparent in the plot.

³ Since the plots correlate, it is only a matter of getting scale and translation right to get the correct zero-crossings. Naturally, the exact splines can be retrieved after training, but that is not important for the qualitative argument being made here: We know that the scaling/translation in the exact splines is correct because of the quantitative results.

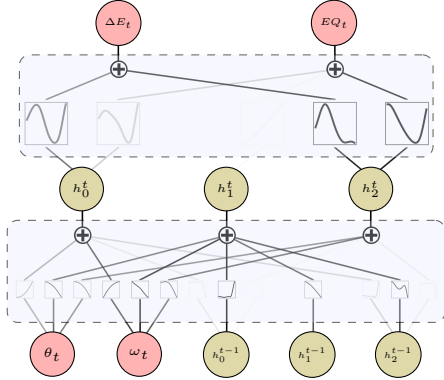


Figure 5: Trained seqKAN/wide model. Unlike seqKAN, it takes only the current ω and θ as inputs and has three hidden-state nodes, giving it room to maintain the previous ω and θ values if the data indicates that this is meaningful.

luxury of having prior knowledge of the correct solution. However, we should note that the analysis is only partially based on prior knowledge: The approximations that led to identifying $(\sin(\theta_t) \cdot \omega_t / \Delta\omega_t)^2$ were guided by the network’s structure and aimed at establishing the validity of the result. In many open-ended tasks the operator is very likely to have similar analytical or experimental tools to test the validity of the dependencies between variables hypothesised by the network.

Which brings us to the second major advantage of the KAN framework: the *controllability* afforded to the operator to manually prune the dependencies that appear to be coincidental. As explained in Section 2.1, the training algorithm is biased towards sparser, less-connected networks and also provides indications about which connections can be safely pruned with minimal loss in performance; This metric is depicted in Figure 3 as darker shades for the connections that the network considers important. Now that we have analysed the network and have established which connections are qualitatively meaningful, we can easily prune those that are not, especially those in lighter shades.⁴

We can now direct our attention to the network learned by seqKAN/wide. If we read Figure 5 we observe that the Energy-Increasing output sums a function over ω_t with a function over the sum $\omega_t + \theta_t$. The network does not utilize any information from the past as the hidden states do not contribute to the recurrency and predictions are made solely based on the current timestep. This analysis is corroborated by the quantitative results in Table 1, where we see that seqKAN/wide perfectly predicts the second label for which only the current input is relevant.

A further observation is that seqKAN/wide ‘wasted’ the extra degrees of freedom afforded to its hidden-state layer to learn a different function for each label instead of forcing the layers to learn functions that contribute to both, as in seqKAN. As a result, it exploited the additional capacity to predict each label independently leading to a distribution of the training loss to different functions, rather than learning more intricate functions that are used for both labels. In essence, the network used the extra capacity not to discover that the inputs should also be carried verbatim to the output layer besides contributing to the hidden-state layer, but to settle for two unconnected theories, one for each label.

As final remark, we will comment on the fact that the additive

⁴ Note that the quantitative results in Table 1 are before any such manual intervention.

functions extracted from KAN networks of splines are a substantial restriction on the shape of the theories that KANs can formulate, and the functions read out of a network need to be understood under this perspective. More concretely, the additive expressions learned by either seqKAN or seqKAN/wide are not, at the surface, similar to the multiplicative expression $(\sin(\theta_t) \cdot \omega_t / \Delta\omega_t)^2$ and the quantitative performance of the seqKAN expression could be considered coincidental. But we should read the comparative analysis of the two networks as revealing that ω^2 captures an essential feature of the phenomenon, which is indeed true as the periods at which squared angular velocity exhibits local maxima correlate with the length of the pendulum string; By contrast, the $\omega_t + \theta_t$ expression learned by seqKAN/wide does not. We will revisit this point in our discussion of the capabilities and limitations of KANs in Section 5.

4.3 Comparative Results

In the previous section, we utilized the formulas that compute the labels of the predictive tasks to perform an analysis on the relevance of the network’s findings. However, in machine learning terms, we have a dual classification task with two binary labels: whether the pendulum’s energy increases or whether it is close to the equilibrium point. Thus, to compare the results across both interpolation and extrapolation tasks for different architectures we use *Receiver Operating Characteristic-Area Under the Curve (ROC-AUC)* and *Precision-Recall-Area Under the Curve (PR-CURVE AUC)* as the evaluation metrics, since they provide a global assessment of the models’ performance without depending on specific thresholds. This choice aligns with our goal of demonstrating the advantages of our model as a general architecture, rather than a specific system solving a specific task. However, when comparing our model to symbolic regression, we are forced to use F1-score since symbolic regression does not output a probability distribution.

In comparing the performance of various sequence processing algorithms, as shown in Table 1a, all models generalize well on the interpolation task. This is a positive and expected outcome, as it suggests that all models are capable of capturing the core structure of the problem. However, with the exception of seqKAN, all models perform significantly worse on the extrapolation task, particularly when predicting the challenging Energy-Increasing label, as seen in Table 1b. seqKAN, on the other hand, maintains consistently high performance metrics, indicating that it is the only model that effectively recovers the hidden variable (string length).

The standard sequence processing algorithms, RNN and LSTM, perform similarly, with the LSTM exhibiting slightly better performance. This is expected, as the LSTM, with its cell state, decides which information to retain from the recent or distant past, whereas the RNN updates its history at every timestep. Specifically in our task, we know for instance that $\Delta\omega$ (two steps) is needed in order to make accurate predictions. The LSTM is more capable of discovering such dependencies.

Regarding the TKAN architecture, which combines LSTM and KAN, it is interesting to note that it performs worse than the vanilla LSTM on the interpolation task but similarly on the extrapolation task. Our intuition suggests that this occurs because the addition of KANs to the LSTM’s output prevents the network from overfitting, encouraging it to learn more meaningful patterns. This could explain its consistently average performance on both tasks, by comparison to LSTM’s performance on the interpolated test set caving in on the extrapolated test set. However, we are unable to test this hypothesis, as TKAN is based on an implementation of the KAN layer that does

Table 1: Evaluation of the performance of RNN, LSTM, TKAN, seqKAN/wide and seqKAN models for the dual classification task with the pendulum length changing exponentially and sequence length being 10. The measured metrics are the areas under: (a) the Receiver Operating Characteristic curve (ROC-AUC) and (b) the Precision Recall curve (PR-AUC).

(a) Interpolation						(b) Extrapolation					
METRIC (AUC)	ARCHITECTURE					METRIC (AUC)	ARCHITECTURE				
	RNN	LSTM	TKAN	SEQKAN/WIDE	SEQKAN		RNN	LSTM	TKAN	SEQKAN/WIDE	SEQKAN
ENERGY INCREASING LABEL						ENERGY INCREASING LABEL					
ROC	0.92	0.98	0.77	0.88	0.96	ROC	0.70	0.68	0.71	0.56	0.90
PR	0.80	0.97	0.83	0.84	0.95	PR	0.51	0.59	0.82	0.53	0.90
CLOSE TO EQUILIBRIUM LABEL						CLOSE TO EQUILIBRIUM LABEL					
ROC	1.00	1.00	0.97	0.89	0.98	ROC	0.72	1.00	0.79	1.00	0.98
PR	1.00	1.00	0.93	0.66	0.97	PR	0.89	1.00	0.88	1.00	0.99

Table 2: Evaluation of Symbolic Regression (SR) and seqKAN. In SR, we approximate the functions of the energy, the ω_t , and the θ_t and utilize them to derive the final labels. We present the best performing SR model. The evaluation metric used is the F1 score. In the case of seqKAN, the optimal F1 score was computed from the thresholds of the PR curve. For the first label, the percentage of seqKAN’s PR curve where its F1-score exceeds that of SR is 98.86% in both interpolation and extrapolation cases.

(a) Interpolation			(b) Extrapolation		
METRIC	ARCHITECTURE		METRIC	ARCHITECTURE	
	SYMBOLIC REGRESSION	SEQKAN		SYMBOLIC REGRESSION	SEQKAN
ENERGY INCREASING LABEL			ENERGY INCREASING LABEL		
F1 SCORE	0.47	0.95	F1 SCORE	0.48	0.89
CLOSE TO EQUILIBRIUM LABEL			CLOSE TO EQUILIBRIUM LABEL		
	1.0	0.92		1.0	0.95

not make the learned functions available for plotting.⁵

In our selected task, while symbolic regression is not expected to perform perfectly due to the lack of an analytic solution, it is anticipated to provide relevant results based on its prior knowledge of potential functions for approximating the phenomenon. However, as shown in Table 2, symbolic regression struggles with the difficult task of predicting the increasing energy change in both interpolation and extrapolation scenarios. The symbolic method produces highly intricate formulas that fit the training data too tightly to generalize well. Additionally, in each run, the functions change significantly, which is expected due to the absence of a closed form. These results further support the idea that seqKAN is particularly well-suited for modeling temporal formulas with a mathematical structure, even in the absence of an analytical solution.

5 Conclusions and Future Work

In this paper we presented *seqKAN*, a recurrent KAN architecture for processing sequences. seqKAN is more faithful to the core concept of the KAN framework than alternative proposals for sequence processing as it ports *concepts* from the RNN framework to KAN without directly integrating processing cells or other MLP-inspired structures.

⁵ This is noted as a known issue in the TKAN repository that was unresolved as of writing this text.

This approach is motivated by the need to retain the interpretability and controllability offered by the less distributed nature of KAN parameters, which are diluted when part of the knowledge distilled from the data is represented in highly-distributed MLP representations. In order to demonstrate this advantage, we qualitatively analysed two alternative seqKAN architectures applied on the same sequence processing task, and offered a human-understandable explanation of dependencies between the variables of the task each of the two networks learned.

What is important is that this interpretability was *not* achieved at the expense of quantitative performance, but combined with performance superior to TKAN (an alternative architecture for KAN-based sequence processing), RNN, LSTM, and symbolic regression. The key characteristic of the evaluation task was that it was not stationary but was influenced by an underlying phenomenon represented by a variable that was not directly visible but that could be inferred from the input. From this phenomenon we extracted an interpolation test-set where the hidden variable was within the same value range as during training and an extrapolation test-set where the hidden variable was outside the range seen during training (although still observing the same natural laws). With this experimental setup, we demonstrated that the performance gap between our approach and the systems we compared against *increased* on the extrapolation test-set.

Having said that, the KAN framework (and consequently seqKAN) poses limitations on the theories that can be represented. The most obvious such limitation, as discussed in the final remark of Section 4.2, is the additive form of the network. Although KANs are inspired by the universality of the Kolmogorov-Arnold Theorem, for the reasons discussed in Section 2.1 the representation based on addition and splines is in reality an approximation. Liu et al. [5, Section 2] show that one can achieve arbitrarily low error by stacking multiple KAN layers, but such an approach weakens the clarity of the result and reduces the confidence that a real, causal dependency has been discovered.

This limitation shows us three directions of possible future research: mapping its extent and impact, maximizing the value we can extract despite it, and lifting it. Regarding the first, the KAN framework has attracted considerable attention in a very short time, so we are confident that a community will coalesce around applying KANs to different tasks so that empirical experience can accumulate. Our immediate plan in this respect is to also develop a Transformer-inspired KAN sequence processor and compare seqKAN and the new architecture on both generated and real-world tasks. What is important for such experiments is reading the expressions learned by the networks and reporting on the impact of this representational limitation.

Which relates to the second future research path, which is to develop human-computer interaction methods that can assist with the painstaking process of extracting symbolic expressions from KAN

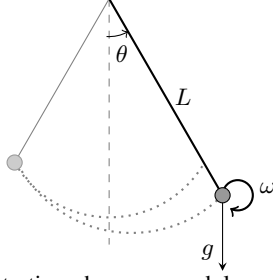


Figure 6: The illustration shows a pendulum with variable length. The equilibrium point is where the string is vertical. θ represents the displacement from equilibrium, while ω is the angular velocity. The pendulum swings between two extreme positions, showing its range of motion, and the length L of the string changes as the pendulum moves, making it time dependent as well.

networks. As there is a delicate balance between over-simplifying what is represented in the network and overwhelming the operator with details, this should be approached in a systematic way involving test operators with varying expertise on KANs.

The final, and most ambitious, goal of generalizing the framework to allow for more complex expressions runs the risk of pushing the framework towards the direction of symbolic regression. Symbolic regression has its own goals and application areas, which are distinct from those of KANs; KAN aims to be a *connectionist* and not a symbolic machine learning framework, and its main juxtaposition is the extremely distributed representation of MLP. In other words, to admin more complex expressions the framework needs to first carry out research on how to prioritize simple addition of learned curves admitting expression complexity only as a last resort. This is an ambitious goal which might require re-thinking foundational aspects of the framework such how back-propagation distributes loss.

A Pendulum with varying string length

A *pendulum* is a mass (referred to as ‘bob’) attached to the end of a string that swings back and forth in a periodic motion under the influence of gravity. The motion of the pendulum is characterized by two key components: the angular displacement θ of the pendulum from the vertical and the angular velocity ω , which is the first derivative of θ (Figure 6).

The motion of a pendulum can be described using a set of equations derived from Newton’s second law of motion and the principles of rotational dynamics. To model the pendulum’s motion over time, we first compute the *angular acceleration* α_t which is proportional to the restoring torque due to gravity:

$$\alpha_t = -\frac{g}{L_t} \sin(\theta_t)$$

where g is the acceleration due to gravity, and L_t is the length of the pendulum at that specific time.

The *angular velocity* ω_t and the angular displacement θ_t are then incrementally computed from their initial values using numerical integration:

$$\begin{aligned} \omega_t &= \omega_{t-1} + \alpha_t \cdot \Delta t \\ \theta_t &= \theta_{t-1} + \omega_t \cdot \Delta t \end{aligned}$$

If we substitute for α_t in the first equation, we can also see that string length can be calculated from displacement and the difference in

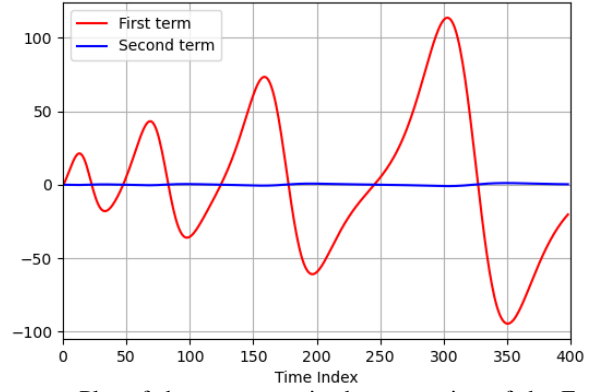


Figure 7: Plot of the two terms in the expression of the Energy-Increasing label. As can be clearly seen, the sum of the two terms is completely dominated by the first term.

velocities between consecutive time steps:

$$\begin{aligned} \Delta\omega &= -\frac{g}{L_t} \sin(\theta_t) \cdot \Delta t \\ L_t &= -\frac{g \sin(\theta_t)}{\Delta\omega/\Delta t} \end{aligned}$$

Our Close-to-Equilibrium binary label is defined by the condition:

$$\theta \cdot \omega \geq 0$$

The total mechanical energy of the pendulum is the sum of kinetic and potential energies, if we assume the mass is concentrated at the end of the pendulum:

$$\begin{aligned} E_t &= \frac{1}{2} m (L_t \omega_t)^2 - mg L_t \cos(\theta_t) \\ &= \frac{1}{2} m \left(\frac{g \sin(\theta_t) \omega_t}{\Delta\omega/\Delta t} \right)^2 + \frac{mg^2 \sin(\theta_t) \cos(\theta_t)}{\Delta\omega/\Delta t} \\ &= \frac{1}{2} m \left(\frac{g \sin(\theta_t) \omega_t}{\Delta\omega/\Delta t} \right)^2 + \frac{mg^2 \sin(2\theta_t)}{2\Delta\omega/\Delta t} \end{aligned}$$

Our Energy-Increasing binary label can then be computed as follows, assuming unit step for all Δt since all our time steps are equal:

$$\Delta \left(\frac{\sin(\theta_t) \omega_t}{\Delta\omega_t} \right)^2 + \Delta \left(\frac{\sin(2\theta_t)}{\Delta\omega_t} \right) \geq 0$$

As can be seen in Figure 7, the sign of the sum of these two Δ terms is completely dominated by the first term. This indicates that a data-driven (as opposed to analytical) model for the Energy-Increasing label that completely ignores the second term should be considered correct.

References

- [1] D. Basina, J. R. Vishal, A. Choudhary, and B. Chakravarthi. KAT to KANs: A review of Kolmogorov-Arnold Networks and the neural leap forward. arXiv:2411.10622 [cs.LG], Nov. 2024. URL <https://arxiv.org/abs/2411.10622>.
- [2] K. Cho, B. van Merriënboer, Çağlar Gülçehre, D. Bahdanau, F. Bougares, H. Schwenk, and Y. Bengio. Learning phrase representations using RNN encoder–decoder for statistical machine translation. In *Proceedings of the 2014 Conference on Empirical Methods in Natural Language Processing (EMNLP)*, 2014. URL <https://doi.org/10.3115/v1/d14-1179>.

- [3] R. Genet and H. Inzirillo. TKAN: Temporal Kolmogorov-Arnold Networks. arXiv:2405.07344v3 [cs.LG], Dec. 2024. URL <https://doi.org/10.48550/arXiv.2405.07344>.
- [4] S. Hochreiter and J. Schmidhuber. Long short-term memory. *Neural Computation*, 9(8), 1997. doi: 10.1162/neco.1997.9.8.1735.
- [5] Z. Liu, Y. Wang, S. Vaidya, F. Ruehle, J. Halverson, M. Soljačić, T. Y. Hou, and M. Tegmark. KAN: Kolmogorov-Arnold Networks. arXiv:2404.19756 [cs.LG], June 2024. URL <https://arxiv.org/abs/2404.19756>.
- [6] J. Schmidt-Hieber. The Kolmogorov-Arnold representation theorem revisited. *Neural Networks*, 137, 2021. doi: 10.1016/j.neunet.2021.01.020.
- [7] R. Tedrake. Underactuated robotics: Algorithms for walking, running, swimming, flying, and manipulation. Course Notes for MIT 6.832, 2023. URL <https://underactuated.csail.mit.edu>.
- [8] A. Vaswani, N. Shazeer, N. Parmar, J. Uszkoreit, L. Jones, A. N. Gomez, Ł. Kaiser, and I. Polosukhin. Attention is all you need. In *Advances in Neural Information Processing Systems 30*, 2017. URL <http://papers.nips.cc/paper/7181-attention-is-all-you-need>.
- [9] G. Yakubu, P. Olejnik, and J. Awrejcewicz. On the modeling and simulation of variable-length pendulum systems: A review. *Archives of Computat Methods Eng*, 29, 2022. URL <https://doi.org/10.1007/s11831-021-09658-8>.